Surface Chemistry

DOI: 10.1002/anie.201200585

The Surface Science Approach for Understanding Reactions on Oxide Powders: The Importance of IR Spectroscopy**

Mingchun Xu, Heshmat Noei, Karin Fink, Martin Muhler, Yuemin Wang, and Christof Wöll**

The role of defects on oxide surfaces, especially that of oxygen defects, has been always considered crucial for the interfacial chemistry of such substrates . Recently, considerable progress has been achieved in this field in particular for the case of titanium dioxide (TiO_2) by the combination of scanning tunneling microscopy (STM) and density functional theory (DFT) calculations. In fact it was possible to study a number of different reactions in considerable detail, including H_2O dissociation,[1,2] O_2 dissociation,[2–4] and (de-)hydrogenation reactions of aromatic compounds.[5]

Unfortunately, the experimental technique upon which this progress is largely based, STM, cannot be applied to powders, the technologically most important form of oxide materials. Although STM investigations of nanometer-sized powder particles have been reported in a (fairly small) number of cases,[6] the investigation of chemical reactions on oxide surfaces and the role of oxygen vacancies cannot be studied for nanoparticles in a straightforward fashion. On the other hand, infrared (IR) spectroscopy has been extensively applied to metal oxide powder samples,[7] but IR results on single-crystal oxides are rather scarce. As a result, the so-called surface science approach, which has been extremely successful for unraveling the mechanism of reactions on metal particles by comparison to results for well-understood single-crystal reference systems,[8] has been severely hampered with regard to understanding reactions on oxide surfaces. Here, we present a novel method capable of investigating oxygen vacancies on surfaces of oxide single crystals as well as on powder particles. We apply this method to demonstrate that the surface chemistry of formaldehyde on TiO_2 nanoparticles is indeed determined by the density of O vacancies. We will first demonstrate that the presence of defect sites on surfaces of rutile TiO_2 (r-TiO_2) can be directly identified by ultrahigh-vacuum IR spectroscopy (UHV-FTIRS) using CO as a probe molecule. After calibrating this method using a well-defined single-crystal r-TiO_2(110) substrate we will apply it to the corresponding powder samples.

The reflection–absorption IR spectroscopy (RAIRS) data shown in Figure 1 demonstrate that on a fully oxidized r-TiO_2(110) surface with a low density of defects only a single band at 2188 cm^{-1} is visible in the CO-stretching regime. This

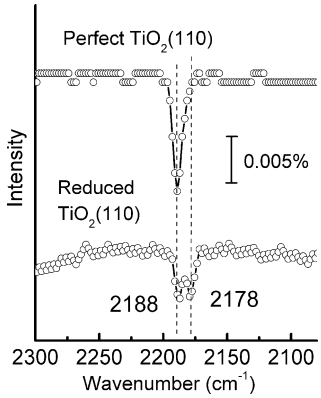

Figure 1. RAIRS data for CO adsorbed on perfect and reduced rutile TiO_2(110) surfaces at 110 K.

frequency is 45 cm^{-1} higher than that observed for the gas phase (2143 cm^{-1}). Such a blue shift is typical for CO adsorbed on oxide surfaces and is in full accord with previous data from electron energy loss spectroscopy (EELS) and theoretical studies for CO adsorbed on the same substrate.[9] When we reduced the TiO_2 surface, either by controlled slightly sputtering or over-annealing at elevated temperatures, a second CO band was observed at 2178 cm^{-1}. In line with a recent STM study on r-TiO_2(110) by Zhao et al.[10] the reduction-induced band at 2178 cm^{-1} is assigned to CO bound to Ti cations located in the vicinity of an oxygen vacancy (i.e. on site 1 indicated in Figure 2), whereas the band at 2188 cm^{-1} is assigned to CO adsorbed on perfect parts of the surface (sites 2–5 in Figure 2). In order to corroborate the assignment of the band at 2178 cm^{-1} we blocked the sites close to the O defects by exposing the substrates to small amounts of O_2 at 110 K. Previous work has shown that under such conditions molecular O_2 adsorbs exclusively at oxygen vacancies.[4,11] As expected, in the IR spectra recorded after such substrates with preadsorbed O_2 were exposed to CO at 110 K, the band

[*] Dr. M. Xu, Dr. Y. Wang
Lehrstuhl für Physikalische Chemie I und
Lehrstuhl für Technische Chemie
Ruhr-Universität Bochum, 44780 Bochum (Germany)
E-mail: wang@pc.rub.de
Dr. H. Noei, Prof. Dr. M. Muhler
Lehrstuhl für Technische Chemie
Ruhr-Universität Bochum (Germany)
Dr. K. Fink
Institut für Nanotechnologie
Karlsruher Institut für Technologie, 76021 Karlsruhe (Germany)
Prof. Dr. C. Wöll
Institut für Funktionelle Grenzflächen
Karlsruher Institut für Technologie, 76021 Karlsruhe (Germany)
E-mail: christof.woell@kit.edu

[**] This research was funded by the German Research Foundation (DFG) within SFB 558 "Metal–Substrate Interactions in Heterogeneous Catalysis". K.F. thanks G. Kresse (Vienna) and M. van Setten (Karlsruhe) for helpful discussions and support on the VASP calculations.

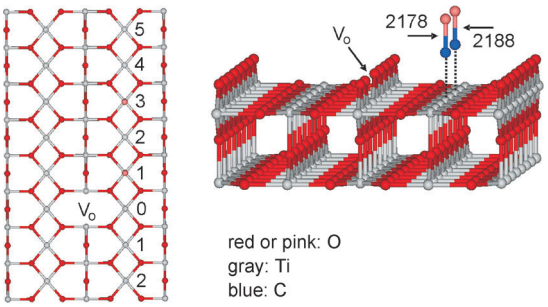

Figure 2. Ball-and-stick model of the rutile TiO_2(110) surface. The CO species adsorbed at different Ti sites (labeled 0–5) are also sketched.

Table 1: Results from DFT calculations for CO adsorbed at different sites in the vicinity of an O vacancy on r-TiO_2(110).[a]

CO site	0	1	2	3	Defect-free
BE[b]	6.31	7.18	7.10	7.15	7.37
BE[10]	7.4	8.8	8.7	8.5	–
ΔBE	0.88	0.00	0.09	0.03	−0.18
$\tilde{\nu}$[c]	2162.5 (2183.4)	2165.3 (2186.2)	2166.2 (2187.1)	2166.9 (2187.8)	2168.7 (2189.7)
$\Delta\tilde{\nu}$	−6.3	−3.4	−2.6	−1.9	0.00

[a] For the labeling of sites see Figure 2. Binding energies are in kcal mol^{-1}, frequencies are in cm^{-1}. [b] This work. [c] The values in parentheses are the results of a normalization procedure using a factor of 1.00965.

at 2178 cm^{-1} was found to be strongly reduced relative to the band at 2188 cm^{-1}.

Figure 3 shows IR data recorded for different CO coverages. Clearly, at low coverage the defect-related band at 2178 cm^{-1} is the dominant one, and only when the intensity of this band approaches saturation does the higher-frequency

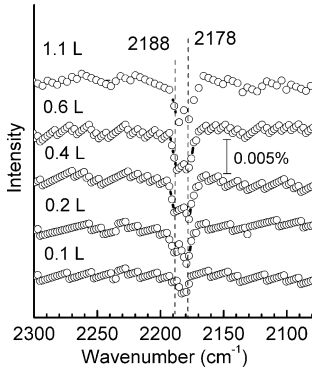

Figure 3. RAIRS data for CO adsorbed on reduced rutile TiO_2(110) surfaces at 110 K as a function of dosage. All spectra were recorded at 110 K with a resolution of 4 cm^{-1} in reflection mode at a grazing incidence of $\theta = 80°$.

band at 2188 cm^{-1} start to grow. This observation is fully consistent with the binding energy for the defect site (site 1 in Figure 2) being about 0.3 kcal mol^{-1} higher than that on the perfect parts of the surface.[10] The slightly higher binding energy close to defects also explains the slight red-shift (ca. 10 cm^{-1}) of the vibration, as expected from Badger's rule.[12]

In addition, we have determined the stretching frequencies of CO adsorbed on the Ti cations labeled 0–2 in Figure 2 and on a perfect TiO_2 surface by DFT calculations using the VASP code.[13] The theoretical results displayed in Table 1 reveal that the stretching frequency for CO adsorbed on ideal Ti^{4+} sites amounts to 2189.7 cm^{-1}. The frequency is thus shifted by 46 cm^{-1} relative to that of free CO, in excellent agreement with the experimentally observed shift and previous studies in which a frequency shift of 50 cm^{-1} was reported.[9] In the theoretical calculations, CO molecules bound at Ti atoms close to the O vacancies exhibit a small red-shift, in good agreement with the experimental data. Note, however, that the absolute value of the shift (3.4 cm^{-1} for position 1 and 2.6 cm^{-1} for position 2) is only a third of the experimental value. Further work will be required in order to find out whether this discrepancy is specific for the particular functional used in these calculations (PBE). Di Valentin et al.[14] showed that the defect electrons of the oxygen vacancy are too delocalized in pure DFT calculations, and hybrid functionals or the use of LSDA + U[15] (local spin density approach with coulomb repulsion) may be necessary for a reliable description. On the other hand, the discrepancies might result from additional charges trapped at the O vacancy not accounted for in the present calculations.

In accord with previous work[10] we conclude that under the present experimental conditions (UHV, substrate temperatures of 110 K), CO does not bind to Ti atoms exposed within the O vacancy, and also not to Ti atoms positioned next to the O vacancy (labeled 0 in Figure 2). As supported by our own calculations, CO will populate only the sites labeled 1 and 2 in Figure 2 (and sites located further away from the oxygen vacancy). On the basis of the intensity ratio of the 2188 cm^{-1} and 2178 cm^{-1} bands in Figure 1 and considering that the maximum coverage of CO on r-TiO_2(110) at 110 K is 0.5 monolayers,[9] the concentration of O vacancies on the reduced r-TiO_2(110) surface is estimated to amount to 10%.

Having demonstrated the validity of our novel method to determine O-vacancy concentrations on r-TiO_2 surfaces, we will now demonstrate the potential of this method for rutile TiO_2 powder particles. After r-TiO_2 powder had been heated in oxygen and then exposed to CO (1×10^{-4} mbar) at 110 K, only one vibrational band at 2184 cm^{-1} is seen (Figure 4), which is assigned to CO molecules bound to ideal Ti^{4+} ions distant to O vacancies or other defects. We applied the same procedure to produce O defects as that employed for the single crystals, namely over-annealing at 900 K in UHV; a weaker, but distinct new band now appears at 2174 cm^{-1}. In accord with the RAIRS data for r-TiO_2(110) single-crystal surfaces, this band is assigned to CO adsorbed on Ti cations proximal to oxygen vacancies (site 1 indicated in Figure 2). From a comparison of the relative intensities of the two bands we conclude that the defect density on the powder particles amounts to about 8%.

After having established a novel, generally applicable method for determining defect densities in a semiquantitative fashion applicable to both single crystals and powders, we demonstrate the potential of this new approach by inves-

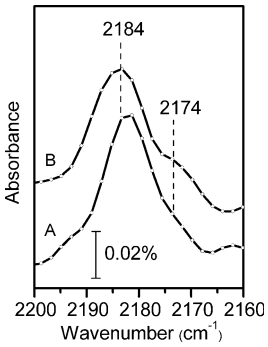

Figure 4. UHV-FTIRS data for CO adsorbed on oxidized and reduced r-TiO_2 powder particles at 110 K recorded in transmission mode: A) Sample was treated with O_2 (5 min, 1×10^{-4} mbar) prior to CO exposure. B) Sample was heated to 900 K in UHV (reduced sample) prior to CO exposure.

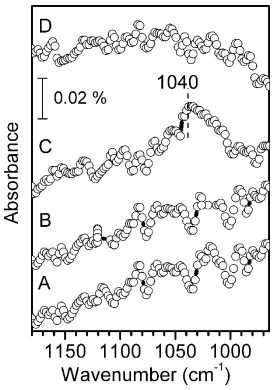

Figure 5. UHV-FTIRS data obtained for r-TiO_2 powder samples. A) Clean r-TiO_2 powder. Powder was B) oxidized and then exposed to formaldehyde (1×10^{-4} mbar) at 400 K, C) reduced and then exposed to formaldehyde (1×10^{-4} mbar) at 400 K. D) The sample from (C) was heated to 600 K before the spectrum was measured. All UHV-FTIR spectra were collected in transmission mode at 110 K.

tigating the reductive coupling of formaldehyde (CH_2O) catalyzed by TiO_2. In a previous study[16] results from HREEL spectroscopy showed that on the perfect r-TiO_2(110) single-crystal surface CH_2O adsorbs weakly in an associative fashion at the Ti^{4+} cations and is released from the surface intact upon heating below 400 K. On the reduced r-TiO_2(110) surface, CH_2O instead binds strongly to O vacancy sites, where a reductive coupling leads to the formation of a diolate species (-OCH_2CH_2O-). Upon heating to about 600 K, this species undergoes deoxygenation and ethylene is observed to desorb from the surface.

RAIRS experiments on differently treated single-crystal r-TiO_2(110) surfaces confirm these earlier findings. After exposure of a fully oxidized substrate (as evidenced by the observation of only one IR band at 2188 cm^{-1}) to CH_2O at 400 K, no adsorbate-induced absorption bands are detected (data not shown). In contrast, UHV-FTIRS results recorded for an over-annealed substrate, where the concentration of O vacancies as estimated from the relative intensity of the defect-induced CO band (see above) amounts to about 10%, reveal a substantial intensity of IR bands which can be assigned to surface-bound diolates formed at O vacancy sites.[16]

We now turn our attention to the reaction on the r-TiO_2 powder samples. Again, IR spectra recorded after exposure of fully oxidized particles to formaldehyde at 400 K only display the features of clean r-TiO_2 nanoparticles (Figure 5B), indicating that CH_2O adsorbed at perfect Ti^{4+} sites is not stable at 400 K, in excellent agreement with the results for the r-TiO_2(110) single-crystal surfaces.

When the r-TiO_2 powder particles were reduced by the over-annealing process described above, the defect density as deduced from the relative intensity of the CO defect band increases to 8%. After exposure of the reduced r-TiO_2 powder particles to formaldehyde at 400 K, a distinct IR band is observed at 1040 cm^{-1} (Figure 5C), which on the basis of the previous data for r-TiO_2(110)[16] can be assigned unambiguously to the C–O stretching vibration within a C_2 diolate species (-OCH_2CH_2O-) formed by activation of formaldehyde at O vacancy sites. Upon heating to 600 K, the diolate-related IR band disappears (see Figure 5D) as a result of ethylene formation.[16]

In conclusion, our high-quality UHV-FTIRS data obtained on r-TiO_2 surfaces of both single crystals and powder particles demonstrate that O vacancy sites formed on reduced TiO_2 can be directly monitored by using CO as a probe molecule. We demonstrate the potential of this novel approach for studying single-crystal surfaces as well as powder particles, by confirming that the conversion efficiency of formaldehyde to ethylene, an important C_1–C_1 coupling reaction, correlates with the density of O vacancies at the surface of r-TiO_2 nanoparticles.

Experimental Section

The UHV-FTIRS experiments on the rutile TiO_2 single-crystal and powder samples were performed in an UHV apparatus, which combines a state-of-the-art vacuum IR spectrometer (Bruker, VERTEX 80v) with a novel UHV system (PREVAC) (for details see Refs. [17,18]). The base pressure in the measurement chamber was 2×10^{-10} mbar. The optical path inside the IR spectrometer and the space between the spectrometer and UHV chamber were evacuated to avoid adsorption of atmospheric moisture, resulting in superior sensitivity and stability of the system.

The single-crystalline r-TiO_2(110) surface was cleaned by several cycles of Ar ion sputtering (2.5 kV, 10 mA) and annealing to 800 K in O_2 atmosphere of 5×10^{-7} mbar in the measurement chamber. The reduced surface was obtained using well-established procedures[17] by controlled slight sputtering or over-annealing to 900 K under UHV conditions. The measurements were performed using RAIRS with a fixed incidence angle of 80°.

The polycrystalline rutile TiO_2 powder samples (Sachtleben, 100 m^2g^{-1}) were first pressed onto a gold-plated stainless-steel grid (0.5×0.5 cm) and then mounted on a sample holder making it possible to record FTIR data in a transmission geometry. It was found crucial to also conduct the powder experiments under UHV conditions. The grid and the attached powder particles were cleaned in the UHV chamber by heating to 700 K in order to remove all contaminations, such as water and hydroxy groups. Prior to each exposure to CO or formaldehyde, a spectrum of the clean powder was recorded as a background reference. All UHV-FTIR spectra were

collected with 1024 scans at a resolution of 4 cm^{-1} in transmission mode.

The DFT Slab calculations were performed using the Vienna ab initio simulation package (VASP)[13] developed at the University of Vienna. The Perdew–Becke–Enzerhoff (PBE) exchange correlation functional[19] and the projected augmented wave method of Blöchl[20] were used in all calculations. A cut-off energy of 400 eV was used throughout. In the *xy* plane a (6×2) unit cell was included and the slab contained four groups of O-Ti-O layers in the *z* direction. Because of the large unit cell, Γ-point approximation was used in all calculations.

The lattice constants were fixed to the values obtained in an optimization for bulk TiO_2 and the atoms of the two lower groups of O-Ti-O layers were kept at bulk positions in all following calculations while the rest of the unit cell was optimized until the forces were less than 0.01 eV $Å^{-1}$. In a second optimization step, the positions of all atoms included in the frequency calculations were optimized with tighter convergence criteria (0.001 eV $Å^{-1}$). Vibrational frequencies were obtained numerically with four different displacements for each coordinate (NFREE = 4). The movements of the CO molecule, the Ti^{4+} adsorption site, and all adjacent O^{2-} ions were considered in the frequency calculations. In the VASP calculations on a free CO monolayer with the lattice constant of the 6×2 unit cell, a frequency of 2122.5 cm^{-1} was obtained for the CO stretching mode. This differs only by 1% from the experimentally observed frequency of 2143 cm^{-1}. In Table 1 the scaled frequencies (scaling factor: 1.00965) are given in brackets.

Received: January 20, 2012
Published online: April 5, 2012

Keywords: defect sites · heterogeneous catalysis · oxides · surface chemistry · vibrational spectroscopy

[1] R. Schaub, P. Thostrup, N. Lopez, E. Laegsgaard, I. Stensgaard, J. K. Norskov, F. Besenbacher, *Phys. Rev. Lett.* **2001**, *87*, 266104; Z. Zhang, O. Bondarchuk, B. D. Kay, J. M. White, Z. Dohnalek, *J. Phys. Chem. B* **2006**, *110*, 21840; A. C. Papageorgiou, N. S. Beglitis, C. L. Pang, G. Teobaldi, G. Cabailh, Q. Chen, A. J. Fisher, W. A. Hofer, G. Thornton, *Proc. Natl. Acad. Sci. USA* **2010**, *107*, 2391.

[2] S. Wendt, R. Schaub, J. Matthiesen, E. K. Vestergaard, E. Wahlstrom, M. D. Rasmussen, P. Thostrup, L. M. Molina, E. Laegsgaard, I. Stensgaard, B. Hammer, F. Besenbacher, *Surf. Sci.* **2005**, *598*, 226.

[3] S. Wendt, P. T. Sprunger, E. Lira, G. K. H. Madsen, Z. S. Li, J. O. Hansen, J. Matthiesen, A. Blekinge-Rasmussen, E. Laegsgaard, B. Hammer, F. Besenbacher, *Science* **2008**, *320*, 1755; O. Bikondoa, C. L. Pang, R. Ithnin, C. A. Muryn, H. Onishi, G. Thornton, *Nat. Mater.* **2006**, *5*, 189.

[4] P. Scheiber, A. Riss, M. Schmid, P. Varga, U. Diebold, *Phys. Rev. Lett.* **2010**, *105*, 216101.

[5] S. C. Li, U. Diebold, *J. Am. Chem. Soc.* **2010**, *132*, 64.

[6] E. Asari, R. Souda, *Surf. Sci.* **2001**, *486*, 203; B. A. Kwetkus, K. Sattler, *Ultramicroscopy* **1992**, *42*, 749.

[7] C. Lamberti, A. Zecchina, E. Groppo, S. Bordiga, *Chem. Soc. Rev.* **2010**, *39*, 4951.

[8] G. Ertl, H. J. Freund, *Phys. Today* **1999**, *52*, 32.

[9] M. Kunat, F. Traeger, D. Silber, H. Qiu, Y. Wang, A. C. van Veen, C. Wöll, P. M. Kowalski, B. Meyer, C. Hattig, D. Marx, *J. Chem. Phys.* **2009**, *130*, 144703.

[10] Y. Zhao, Z. Wang, X. F. Cui, T. Huang, B. Wang, Y. Luo, J. L. Yang, J. G. Hou, *J. Am. Chem. Soc.* **2009**, *131*, 7958.

[11] C. N. Rusu, J. T. Yates, *Langmuir* **1997**, *13*, 4311; M. A. Henderson, W. S. Epling, C. L. Perkins, C. H. F. Peden, U. Diebold, *J. Phys. Chem. B* **1999**, *103*, 5328.

[12] M. T. Green, *J. Am. Chem. Soc.* **2006**, *128*, 1902; K. R. Asmis, G. Meijer, M. Brummer, C. Kaposta, G. Santambrogio, L. Woste, J. Sauer, *J. Chem. Phys.* **2004**, *120*, 6461.

[13] G. Kresse, J. Furthmuller, *Phys. Rev. B* **1996**, *54*, 11169; G. Kresse, D. Joubert, *Phys. Rev. B* **1999**, *59*, 1758.

[14] C. Di Valentin, G. Pacchioni, A. Selloni, *Phys. Rev. Lett.* **2006**, *97*, 166803.

[15] B. J. Morgan, G. W. Watson, *Surf. Sci.* **2007**, *601*, 5034.

[16] H. Qiu, H. Idriss, Y. M. Wang, C. Wöll, *J. Phys. Chem. C* **2008**, *112*, 9828.

[17] M. C. Xu, Y. K. Gao, E. M. Moreno, M. Kunst, M. Muhler, Y. M. Wang, H. Idriss, C. Wöll, *Phys. Rev. Lett.* **2011**, *106*, 0.

[18] H. Noei, C. Wöll, M. Muhler, Y. M. Wang, *J. Phys. Chem. C* **2011**, *115*, 908; Y. Wang, A. Glenz, M. Muhler, C. Wöll, *Rev. Sci. Instrum.* **2009**, *80*, 113108.

[19] J. P. Perdew, K. Burke, M. Ernzerhof, *Phys. Rev. Lett.* **1997**, *78*, 1396.

[20] P. E. Blöchl, *Phys. Rev. B* **1994**, *50*, 17953.

